NANO LETTERS
2008
Vol. 8, No. 7
1991-1994

Ultrafast Spin Dynamics in Colloidal ZnO Quantum Dots

Nils Janßen,[†] Kelly M. Whitaker,[‡] Daniel R. Gamelin,[‡] and Rudolf Bratschitsch*,[†]

Department of Physics and Center for Applied Photonics, University of Konstanz, D-78464 Konstanz, Germany, and Department of Chemistry and Center for Nanotechnology, University of Washington, Seattle, Washington 98195

Received April 14, 2008; Revised Manuscript Received May 30, 2008

ABSTRACT

Time-resolved Faraday rotation measurements in the ultraviolet have been performed to reveal the ultrafast spin dynamics of electrons in colloidal ZnO quantum dots. Oscillating Faraday rotation signals are detected at frequencies corresponding to an effective g factor of $g^* = 1.96$. Biexponential oscillation decay is observed that is due to (i) rapid depopulation of the fundamental exciton ($\tau = 250$ ps) and (ii) slow electron spin dephasing ($T_2^* = 1.2$ ns) within a metastable state formed by hole-trapping at the quantum dot surface.

Electrons confined within semiconductor quantum dots (QDs) have generated a great deal of interest recently, motivated in part by proposals to use quantum-confined electron spins for quantum information processing.[1] The wide-bandgap semiconductor ZnO possesses both a large bandgap of 3.4 eV and an exciton binding energy of 60 meV, which will be strongly beneficial to room-temperature operation of future spintronic devices made of this material. Colloidal ZnO QDs have been synthesized by a wide variety of methods. Electrochemical and photochemical techniques have been developed that allow for the introduction of quantum-confined electrons into these QDs.[2–9] These electrons have been studied by optical,[2–5,8,9] electrochemical,[2,3,6,7] and magnetic resonance techniques.[8,9] For example, the new near-infrared electronic absorption band that appears with ZnO QD charging and that is accompanied by bleaching of the band gap absorption edge has been attributed to intra-conduction-band electron excitation.[2–5] Optical measurements performed in conjunction with electrochemical reduction of ZnO QD films have been interpreted to suggest staircase filling of the ZnO QD conduction band with multiple electrons.[6] The added electrons also possess interesting spin properties that have been probed by electron paramagnetic resonance (EPR) spectroscopy.[8,9] EPR experiments on such charged colloidal ZnO quantum dots have shown size-dependent g^* values that confirm electron delocalization throughout the QDs. An analysis of the EPR linewidths revealed relatively slow electron spin dephasing even at room temperature. EPR line width measurements as a function of ZnO QD isotope content confirmed association of spin dephasing with the electron−nuclear hyperfine interaction involving the ^{67}Zn ($I = 5/2$) isotope. Magnetic exchange interactions between conduction band electrons and magnetic dopants were also probed by EPR spectroscopy.[9]

A leading technique for studying carrier spin dynamics in QDs directly in the time domain is time-resolved Faraday rotation (TRFR) spectroscopy. In this pump−probe technique, carriers are both generated and probed using ultrafast laser pulses in resonance with the fundamental absorption edge of the bulk semiconductor or with confined energy levels in semiconductor nanostructures.[10–12] In related studies, TRFR has previously been applied to study epitaxial *n*-type ZnO films, where ensemble electron spin dephasing times up to $T_2^* = 2$ ns at 10 K were measured.[13] TRFR has also been applied previously to study coherent spin dynamics in colloidal CdSe and related chalcogenide nanocrystals.[14–16]

In this letter, we describe the application of TRFR spectroscopy in the ultraviolet to reveal the ultrafast spin dynamics of electrons in colloidal ZnO QDs. Oscillating Faraday rotation amplitudes are observed at frequencies indicative of $g^* = 1.96$, consistent with previous magnetic resonance results for electrons in colloidal ZnO QDs.[8,9] Biexponential oscillation decay is observed that is due to (i) rapid depopulation of the fundamental exciton and (ii) slow dephasing of electron spins when holes are trapped at the quantum dot surfaces. To our knowledge, these results represent the first successful application of direct time-resolved spin coherence probes to ZnO nanocrystals or to oxide nanocrystals in general. The results show that metastable charge-separated states can dominate the ultrafast spin dynamics of such semiconductor QDs, raising new possibilities for controlling spins in semiconductor nanostructures via charge separation.

---

* Corresponding author. E-mail: Rudolf.Bratschitsch@uni-konstanz.de.
[†] University of Konstanz.
[‡] University of Washington.

10.1021/nl801057q CCC: $40.75

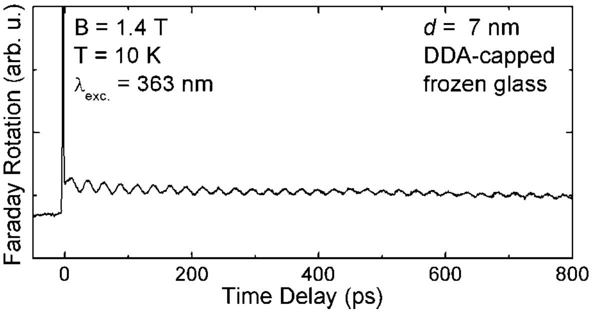

Figure 1. Time-resolved Faraday rotation signal for ~7-nm-diameter colloidal ZnO quantum dots, recorded at a transverse magnetic field of 1.4 T and a temperature of 10 K.

Freestanding ZnO QDs of 7.0 ± 1.7 nm diameter capped with either trioctylphosphine oxide (TOPO) or dodecylamine (DDA) were prepared as colloidal suspensions in toluene and characterized as described previously.[17] For TRFR measurements, thin films of these ZnO colloids were deposited by drop-coating onto sapphire substrates, forming glasses within a frozen matrix of the surface capping ligand. Samples best suited for TRFR studies were found empirically to have transmittance of ca. 0.3−0.4 at the midpoint and the minimum amount of scattering. Qualitatively similar results were found for both TOPO and DDA surface-capping ligands. In the TRFR experiment, spin-polarized electrons and holes are optically excited by a circularly polarized laser pulse resonant with the fundamental bandgap in the UV. Subsequently, carriers precess coherently in a transversely applied magnetic field (Larmor spin precession). By measuring the polarization rotation of a linearly polarized probe beam transmitted through the sample, one is able to monitor the carrier spin precession over time. Spectrally narrow pump and probe pulses in the UV ($\Delta\lambda_{\mathrm{fwhm}} = 0.2$ nm) were generated by frequency-doubling picosecond light pulses from a Coherent MIRA 900 Ti:sapphire oscillator in nonlinear BiB_3O_6 (BiBo) crystals. The pump beam was switched between left and right circular polarization with a photoeleastic modulator operating at 84 kHz. Transient Faraday rotation signals were recorded with an optical polarization bridge and lock-in detection.

Figure 1 shows the TRFR signal obtained for an ensemble of colloidal ZnO QDs held at a temperature of 10 K in a transverse magnetic field of 1.4 T. Following a large positive signal at zero time delay, sinusoidal oscillations with a frequency of 38.5 GHz are observed on top of a step offset. In the simplest case, the oscillatory component is associated with spin precession that decays as a function of time as described by eq 1. T_2* is the ensemble spin dephasing time constant, ω_L is the Larmor precession frequency, and C is a constant related to the amplitude of spin polarization.

$$\theta_F(t) = C\cos(\omega_L t)e^{-t/T_2^*} \tag{1}$$

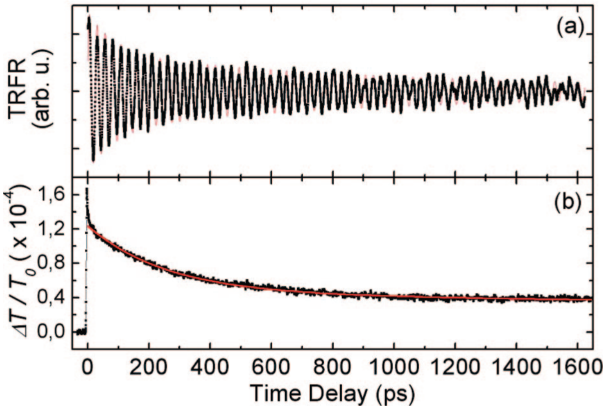

Figure 2. (a) Oscillatory time-resolved Faraday rotation signal extracted from Figure 1 (red line: biexponentially decaying sinusoidal fitting function). (b) Time-resolved differential transmission signal of the colloidal ZnO QDs, measured under essentially identical experimental conditions (red line: biexponentially decaying fitting function)

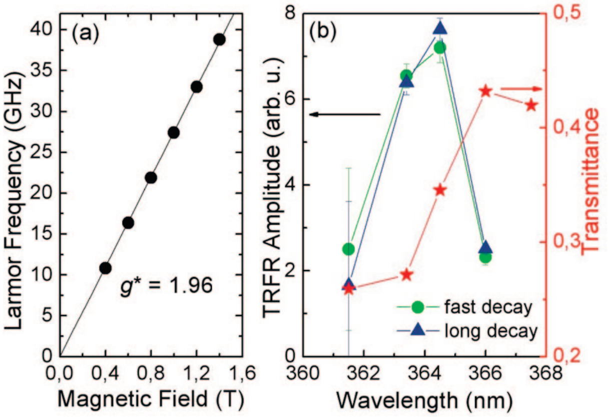

Figure 3. (a) Magnetic field dependence of the TRFR oscillatory frequency of 7-nm-diameter ZnO QDs at 10 K, with linear fit yielding $g^* = 1.96$. (b) Wavelength dependence of the amplitude of the Faraday rotation signal (circles and triangles for fast and slow decaying component). Transmittance of the sample, showing the absorption band edge of the fundamental bandgap (stars).

To analyze the oscillations, we removed the slowly varying baseline. Sine-wave fitting of the oscillating signal in Figure 2a reveals that the amplitude decay is not single but biexponential, with two very different decay timescales. A fast decay with a time constant on the order of 100 ps is followed by slow decay that reflects spin coherence exceeding one nanosecond (~1.2 ns).

Figure 3a shows a linear dependence of the oscillation frequency on magnetic field. The slope of the best fit line yields $g^* = 1.96$ according to eq 2,

$$g^* = \frac{\hbar\omega_L}{\mu_B B} \tag{2}$$

in agreement with previous magnetic resonance investigations on similar colloidal ZnO QDs.[8,9]

To understand the observed biexponential decay, complementary transient differential transmission measurements were performed, which revealed the ultrafast population dynamics in the ZnO dots following UV excitation. The sample and the experimental conditions in this ultrafast pump−probe experiment were essentially the same as for the TRFR study. Representative transient differential transmission data are presented in Figure 2b. The data show an increase in transmission induced by the pump pulse, followed

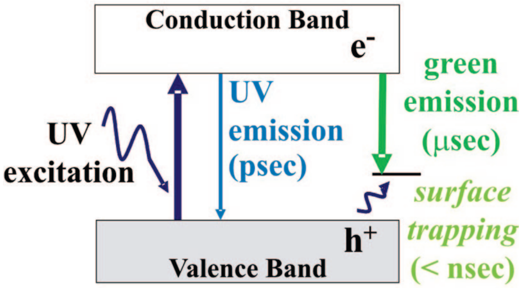

Figure 4. Schematic representation of the kinetic processes following photoexcitation of colloidal ZnO QDs. The fast and slow TRFR decay processes are associated with (i) decay of the UV-emitting (fundamental exciton) state and (ii) spin-dephasing of electrons within the green-emitting (hole-trapped) state, respectively.

by absorption recovery. As with the TRFR oscillation amplitudes, the transient transmission data show two recovery time scales, $\tau_1 \approx 250$ ps and $\tau_2 \geq 7$ ns. The amplitudes of the two components are approximately equal. Because these transients were collected at the ZnO absorption band edge, both decay processes are definitively associated with charge carriers within the band structure of the ZnO QDs, since only these result in band edge bleaching. As illustrated in Figure 3b, detuning the pump/probe wavelength to either above or below the band edge results in a strong decrease of the oscillation amplitude.

The fast decay process (τ_1) seen in Figure 2a and b is associated with rapid depopulation of the UV-emitting excited-state of the ZnO QDs. Previously, a 90 ps UV emission decay was observed at room temperature in bulk ZnO samples with a UV photoluminescence quantum yield of ~0.016.[18] A UV emission decay of <300 ps at 30 K has also been reported for ZnO QDs.[19] Both timescales are in good agreement with our measured fast decay time τ_1. The associated UV emitting state has been described previously as a shallow-trapped exciton involving shallow electron traps that do not lead to electron localization.[20] Nonradiative processes dominate the kinetics of relaxation from this state in ZnO QDs. For similar colloidal ZnO QDs, a nonradiative decay rate constant of $\sim 10^{12}$ s^{-1} has been estimated from steady-state UV photoluminescence quantum yields ($\sim 2 \times 10^{-4}$).[17] Among the various nonradiative decay pathways depopulating this UV state, hole localization at deep traps is the best understood. The broad visible luminescence that often dominates the photoluminescence of ZnO QDs has been assigned to recombination of conduction-band-like electrons with such deeply trapped holes.[20] Figure 4 summarizes the main photophysical processes related to both UV and visible luminescence in ZnO QDs. Because this visible luminescence is sensitive to surface modification, specifically to OH^- functionalities,[17,21] it likely involves hole-trapping at the QD surfaces. Consistent with this interpretation, when ZnO QDs are excited in the presence of a hole scavenger such as EtOH, the hole can be removed from the surface leaving the conduction-band-like electron behind; this is the motif that has been studied by EPR spectroscopy.[8,9] Overall, these considerations support the conclusion that the fast decay component τ_1 observed in both the TRFR and differential transmission measurements (Figure 2a and b) is determined predominantly by nonradiative depopulation of the UV emitting state, including by hole-trapping. Hence, the TRFR oscillation decay mainly reflects the decreasing population of oscillating electrons and not pure spin-dephasing T_2*. In fact, the fast decay times observed with TRFR (100 ps) and differential transmission (250 ps) are of the same order of magnitude, but not exactly the same. A plausible reason that the times are similar, but the spin decay is slightly faster than the population decay, may be an additional fast spin-dephasing mechanism operative in the first 100 ps. For example, efficient electron−hole spin scattering would be present only during that time, when the hole has neither recombined nor been trapped at the dot surface.

The second, slower decay in the TRFR signal is on the order of a nanosecond and is directly related to the metastable hole-trapped excited state. As described above, the hole of the optically generated electron−hole pair is trapped effectively on the dot surface. This process leaves the electron behind in the ZnO dot core. This electron is conduction-band-like, as has been confirmed in experiments on ZnO QDs of different sizes, in which the visible photoluminescence emission wavelength followed the size dependence anticipated from the electron effective mass in ZnO.[22] The precession of this electron in the transverse magnetic field gives rise to the observed Faraday rotation signal with the slow decay time. This interpretation is confirmed by the differential transmission data of Figure 2b, which indicate a slow second decay process ($\tau_2 \gg 1$ ns). Earlier time-resolved photoluminescence measurements have shown lifetimes of several hundred nanoseconds to microseconds for this state.[20] Recombination of the hole-trapped species is thus slow relative to electron spin-dephasing. The observed oscillatory decay therefore reflects the intrinsic spin-dephasing dynamics (T_2*) of the conduction-band electron in this configuration, and not the population decay dynamics. T_2* is the ensemble spin-dephasing time, which may be limited by the distribution of *g*-factors because of inhomogeneities in size and shape of the different dots. However, g* is not highly sensitive to diameter in ZnO dots within the 7.0 ± 1.7 nm range investigated here. From EPR data (not shown), we estimate a Δg of 0.004 for the whole distribution. However, we use narrowband picosecond laser pulses in the TRFR experiment ($\Delta\lambda_{\text{fwhm}} = 0.2$ nm), which excite and probe only a small subensemble.[23] In our case, this results in a small Δg of ~0.0002 and hence a calculated[24] T_2* time of 57 ns for a magnetic field of 1.4 T in the limit of T_2* coming entirely from *g*-value inhomogeneity. This value is substantially higher than our measured value of 1.2 ns. Another important dephasing mechanism in ZnO quantum dots is electron−nuclear hyperfine coupling involving ^{67}Zn ($I = 5/2$, natural abundance of 4.1%). The importance of hyperfine contributions is confirmed by the observation of nearly Lorentzian lineshapes having a clear dependence on ^{67}Zn content in the EPR spectra of related charged colloidal ZnO QDs.[8] Further studies are needed to unambiguously identify the relative contributions of the different spin-dephasing processes.

Interestingly, because the decay of the hole-trapped species is also slow compared to the time between the successive laser pulses of 13 ns ($\tau_{\mathrm{rep}} = 76$ MHz) in the TRFR experiment, a steady-state population of one-electron-charged ZnO QDs must exist. This situation may relate to experiments on self-assembled InAs quantum dots, where only singly charged quantum dots caused an oscillatory TRFR signal.[23] Finally, it is noted that the occurrence of both fast and slow TRFR oscillations at the same center frequency, which corresponds to $g^* = 1.96$, supports the assertion that no major change in the electron's wave function occurs upon hole trapping; that is, the electron in the hole-trapped state remains conduction-band-like.

In summary, ultrafast spin dynamics in colloidal ZnO quantum dots have been measured for the first time using time-resolved Faraday rotation spectroscopy in the ultraviolet. Although the fast excitonic spin decay is governed by the short lifetime of this excited state, the deep trap state is extremely long-lived and allows for the direct observation of spin-dephasing of conduction-band electrons in the colloidal ZnO dots. The values for T_2^* and g^* measured by time-resolved Faraday rotation spectroscopy are consistent with those reported for photochemically charged colloidal ZnO QDs determined by EPR spectroscopy in the frequency domain.[8,9] Our results reveal that metastable charge-separated excited states offer interesting possibilities for the control and study of carrier spin dynamics in semiconductor nanostructures. Beyond the surface-hole-trapping explored here for ZnO nanocrystals, more sophisticated strategies for achieving photoinduced charge separation in colloidal nanostructures may also be envisioned, for example those involving quasi-type-II or related nanoheterojunctions.[25,26] Further coupling of such colloidal nanostructures with high-quality nanophotonic architectures[27–30] can be anticipated to generate new approaches for all-optical spin-based information processing.

Acknowledgment. We thank Tobias Hanke, Florian Sotier, and Tim Thomay for their help with sample preparation. R.B. acknowledges the continuous support of Alfred Leitenstorfer and Ulrich Rüdiger. Financial support from the Deutsche Forschungsgemeinschaft (DFG) through SFB 513 and the priority program SPP1285, the Kompetenznetz Funktionelle Nanostrukturen Baden-Württemberg, and a grant from the Ministry of Science, Research, and Arts Baden-Württemberg, as well as from the US NSF (CRC-0628252 to DRG and DGE-0504573 (IGERT fellowship) to K.M.W.), the Research Corporation, the Dreyfus Foundation, and the Sloan Foundation is gratefully acknowledged. R.B. acknowledges the support of the Center for Junior Research Fellows of the University of Konstanz.

References

(1) Cerletti, V.; Coish, W. A.; Gywat, O.; Loss, D. *Nanotechnology* **2005**, *16*, R27–R49.

(2) Haase, M.; Weller, H.; Henglein, A. *J. Phys. Chem.* **1988**, *92*, 482–487.

(3) Hoyer, P.; Weller, H. *Chem. Phys. Lett.* **1994**, *221*, 379–384.

(4) Shim, M.; Guyot-Sionnest, P. *J. Am. Chem. Soc.* **2001**, *123*, 11651–11654.

(5) Germeau, A.; Roest, A. L.; Vanmaekelbergh, D.; Allan, G.; Delerue, C.; Meulenkamp, E. A. *Phys. Rev. Lett.* **2003**, *90*, 097401.

(6) Roest, A. L.; Kelly, J. J.; Vanmaekelbergh, D.; Meulenkamp, E. A. *Phys. Rev. Lett.* **2002**, *89*, 036801.

(7) Roest, A. L.; Germeau, A.; Kelly, J. J.; Vanmaekelbergh, D.; Allan, G.; Meulenkamp, E. A. *Chem. Phys. Chem.* **2003**, *4*, 959–966.

(8) Liu, W. K.; Whitaker, K. M.; Smith, A. L.; Kittilstved, K. R.; Robinson, B. H.; Gamelin, D. R. *Phys. Rev. Lett.* **2007**, *98*, 186804.

(9) Liu, W. K.; Whitaker, K. M.; Kittilstved, K. R.; Gamelin, D. R. *J. Am. Chem. Soc.* **2006**, *128*, 3910–3911.

(10) Awschalom, D. D.; Loss, D.; Samarth, N. *Semiconductor Spintronics and Quantum Computation*; Springer-Verlag: Heidelberg, 2002.

(11) Bratschitsch, R.; Chen, Z.; Cundiff, S. T.; Zhukov, E. A.; Yakovlev, D. R.; Bayer, M.; Karczewski, G.; Wojtowicz, T.; Kossut, J. *Appl. Phys. Lett.* **2006**, *89*, 221113.

(12) Chen, Z.; Carter, S.; Bratschitsch, R.; Dawson, P.; Cundiff, S. T. *Nat. Phys.* **2007**, *3*, 265.

(13) Ghosh, S.; Sih, V.; Lau, W. H.; Awschalom, D. D.; Bae, S.-Y.; Wang, S.; Vaidya, S; Chapline, G. *Appl. Phys. Lett.* **2005**, *86*, 232507.

(14) Gupta, J. A.; Awschalom, D. D.; Peng, X.; Alivisatos, A. P. *Phys. Rev. B* **1999**, *59*, R10421–R10424.

(15) Gupta, J. A.; Awschalom, D. D.; Efros, A. L.; Rodina, A. V. *Phys. Rev. B* **2002**, *66*, 125307.

(16) Berezovsky, J.; Gywat, O.; Meier, F.; Battaglia, D.; Peng, X.; Awschalom, D. D. *Nat. Phys.* **2006**, *2*, 831.

(17) Norberg, N. S.; Gamelin, D. R. *J. Phys. Chem. B* **2005**, *109*, 20810–20816.

(18) Schubnell, M.; Kamber, I.; Beaud, P. *Appl. Phys. A: Mater. Sci. Process.* **1997**, *64*, 109–113.

(19) Yamamoto, S.; Yano, H.; Mishina, T.; Nakahara, J. *J. Lumin.* **2007**, *126*, 257–262.

(20) van Dijken, A.; Meulenkamp, E. A.; Vanmaekelbergh, D.; Meijerink, A. *J. Phys. Chem. B* **2000**, *104*, 1715–1723.

(21) Zhou, H.; Alves, H.; Hofmann, D. M.; Kriegseis, W.; Meyer, B. K.; Kaczmarczyk, G.; Hoffmann, A. *App. Phys. Lett.* **2002**, *80*, 210–212.

(22) van Dijken, A.; Meulenkamp, E. A.; Vanmaekelbergh, D.; Meijerink, A. *J. Lumin.* **2000**, *90*, 123.

(23) Greilich, A.; Oulton, R.; Zhukov, E. A.; Yugova, I. A.; Yakovlev, D. R.; Bayer, M.; Shabaev, A.; Efros, Al., L.; Merkulov, I. A.; Stavarache, V.; Reuter, D.; Wieck, A. *Phys. Rev. Lett.* **2006**, *96*, 227401.

(24) Kikkawa, J.; Awschalom, D. D. *Phys. Rev. Lett.* **1998**, *80*, 4313.

(25) Kraus, R. M.; Lagoudakis, P. G.; Rogach, A. L.; Talapin, D. V.; Weller, H.; Lupton, J. M.; Feldmann, J. *Phys. Rev. Lett.* **2007**, *98*, 017401.

(26) Piryatinski, A.; Ivanov, S. A.; Tretiak, S.; Klimov, V. I. *Nano Lett.* **2007**, *7*, 108–115.

(27) Poitras, C. B.; Lipson, M.; Du, H.; Hahn, M. A.; Krauss, T. D. *Appl. Phys. Lett.* **2003**, *82*, 4032.

(28) Li, Y. Q.; Steuerman, D. W.; Berezovsky, J.; Seferos, D. S.; Bazan, G. C.; Awschalom, D. D. *Appl. Phys. Lett.* **2006**, *88*, 193126.

(29) Kahl, M.; Thomay, T.; Kohnle, V.; Beha, K.; Merlein, J.; Hagner, M.; Halm, A.; Ziegler, M.; Nann, T; Fedutik, Y.; Woggon, U.; Artemyev, M.; Pérez-Willard, F.; Leitenstorfer, A.; Bratschitsch, R. *Nano Lett.* **2007**, *7*, 2897–2900.

(30) Merlein, J.; Kahl, M.; Zuschlag, A.; Sell, A.; Halm, A.; Boneberg, J.; Leiderer, P.; Leitenstorfer, A.; Bratschitsch, R. *Nat. Photon.* **2008**, *2*, 230.

NL801057Q